J Mater Sci: Mater Electron (2017) 28:12356–12362
DOI 10.1007/s10854-017-7055-7

Effects of annealing temperature, ambient humidity and temperature on dielectric properties of sol–gel-derived amorphous alumina thin film

Zhen Su[1] · Manwen Yao[1] · Jianwen Chen[1] · Xi Yao[1]

Received: 25 February 2017 / Accepted: 29 April 2017 / Published online: 8 May 2017

Abstract Alumina is the great potential material for the high-energy-storage application. Annealing temperature, ambient humidity and temperature are crucial parameters for further investigations of alumina dielectrics. Highly dense and uniform amorphous alumina thin films were prepared by sol–gel and spin-coating technology. The effects of annealing temperature, relative ambient humidity and temperature on dielectric properties of amorphous alumina thin films were first investigated. The annealing temperature varied from 450 to 700 °C. The ambient humidities of 20, 40, 60 and 80% were chosen. The leakage current density of film annealed at 450 °C showed strong dependence on the ambient humidity. However, the effect of ambient humidity on leakage current density weakened as the annealing temperature rising. At the constant ambient humidity, films annealed at 450 and 500 °C showed lower leakage current densities than films annealed at 600 and 700 °C. The various annealing temperatures made little influence on dielectric loss but can enhance slightly the dielectric constant at 500 °C. The annealing temperature of 500 °C was reasonable and the resulting films exhibited stable conduction mechanism at various ambient temperatures. Moreover, the annealing temperature, ambient humidity and temperature did not make the remarkable influence on the breakdown strength.

✉ Manwen Yao
yaomw@tongji.edu.cn

Zhen Su
18901998729@126.com

[1] Functional Materials Research Laboratory, School of Materials Science & Engineering, Tongji University, No. 4800 Cao'an Road, Shanghai 201804, China

1 Introduction

Alumina is a technically important material and widely used in variety of applications, such as corrosion protections [1, 2], thermometry sensors, catalyst supports [3], electrical insulators and dielectric resonators [4], due to its outstanding electrical, optical, chemical and thermal properties [5]. As a dielectric material, alumina presents the key properties of high dielectric constant and dielectric strength from DC to GHz frequencies [6] and has been caused considerable attentions to explore its potential application for high-energy-storage capacitors. As is well known, the energy storage density is proportional to the dielectric constant and the square of breakdown strength. Moreover, leakage current and dielectric breakdown strength play an important role in determining the reliability of electric devices. Hence, the leakage current, breakdown strength and dielectric constant are critical factors for the energy storage dielectrics [7].

Alumina has the particularity of existing in various metastable phases, such as γ-, δ-, η-, θ-, χ- and α-Al_2O_3 as well as the amorphous phase. They are classified in terms of the oxygen sublattice structure and the distribution of aluminum ions into the tetrahedral and octahedral interstitial sites [8]. Typically, the amorphous alumina adheres to the substrate well [9] and embraces higher activity. Various deposition techniques have been employed for preparing amorphous alumina thin film, including magnetron sputtering [10], oxygen-ion assisted deposition [11], electron beam evaporation [12], atomic layer deposition [13, 14], chemical vapor deposition [15] and sol–gel [16]. The sol–gel technology is mainly based on a succession of hydrolysis-condensation reactions at moderate temperature to prepare networks and provides distinct advantages over the other methods, such as controlling over

composition, homogeneity and purity at the lower processing temperature.

The element doping effect on dielectric properties of amorphous alumina thin film has been investigated [16, 17]. However, the effects of annealing temperature, ambient humidity and temperature on dielectric properties for the undoped amorphous alumina thin film have not been achieved. Taking the above factors into account is inevitable and essential in the process of investigating dielectric properties of the undoped alumina thin film. The annealing temperature is responsible for the microstructural transition, which play a key role in determining dielectric properties. The ambient humidity and temperature affects the reliability of alumina dielectrics.

The paper aims to clarify the influence of annealing temperature, ambient humidity and temperature on dielectric properties of sol–gel-derived amorphous alumina thin film at high electric field. And the results shed more light on further investigations of the alumina thin film.

2 Experimental

2.1 Preparation of the alumina thin film

Alumina thin films were prepared according to the following procedures by sol–gel and spin coating technology: (a) 0.02 mol aluminum isopropoxide was dissolved in 50 ml of glycol ether with stirring at 60 °C for 30 min on the magnetic stirrer; (b) the aluminum isopropoxide solution was mixed with 0.02 mol acetylacetone with stirring for 30 min; (c) 10 ml acetic acid as catalyst was added to the above solution at 90 °C with agitation for 30 min to get a clear and homogeneous sol; (d) thin films were deposited on Pt/Ti/SiO_2/Si substrates on layer-by-layer application by spin-coating method in a clean-room environment; (e) films were annealed at 450, 500, 600 and 700 °C (represented as T-450, T-500, T-600 and T-700), respectively, for 180 min with a heating speed of 3 °C/min in a conventional furnace and then cooled down to the room temperature. For the electrical measurement, Au top electrodes with the diameter of 1 mm were fabricated onto alumina thin films by ion sputtering.

2.2 Characterizations

The glancing-angle X-ray diffraction with an incident angle of 1° to the film surface (XRD, Rigaku D/max-2550, USA) was used to identified the phase. The chemical bonds were analyzed through fourier transform infrared spectroscopy (FT-IR, EQUINOX 55, Bruker Optics, Germany). Surface characteristics were observed by field emission scanning electron microscopy (FESEM, S-4700, Hitachi, Japan) and atomic force microscope (AFM, SPA-300HV, NSK, Japan). J (current density)–E (electric field) characteristics were measured by the Keithley 2400 source meter unit. The dielectric constant and dielectric loss were measured from 200 kHz to 2 MHz using a LCR meter (E4980A, Agilent, USA). Thin films were placed in constant temperature and constant relative humidity box for 180 min prior to J–E, dielectric constant and dielectric loss measurements. The thickness of thin films measured by a dual bean laser interferometer (Filmetrics F20, San Diego, CA) was about 210 nm.

3 Results and discussion

3.1 Phase structure and surface morphology

According to the TG-DSC results in the previous work [17], we have known that organics are almost combusted completely at ~450 °C in the alumina xerogel and the primary crystallization reactions dominate in the temperature range of 875–1200 °C. In order to ensure that the films present amorphous phase with the least number of residual organics, the ultimate annealing temperatures of 450, 500, 600 and 700 °C are chosen to investigate the effect of annealing temperature on structure and morphology.

Figure 1 depicts XRD patterns of alumina thin films annealed at 450, 500, 600 and 700 °C. No crystallization peak is observed indicating alumina thin films are amorphous.

Figure 2 shows the FT-IR curves of T-450, T-500, T-600 and T-700 samples. In each FT-IR spectrum, a strong absorption band dominates in the frequency range of 3000–4000 cm^{-1}. These are the stretching vibration

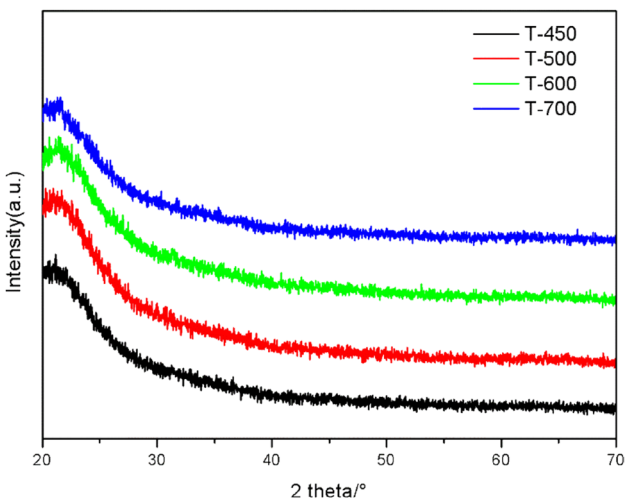

Fig. 1 XRD patterns of T-450, T-500, T-600 and T-700

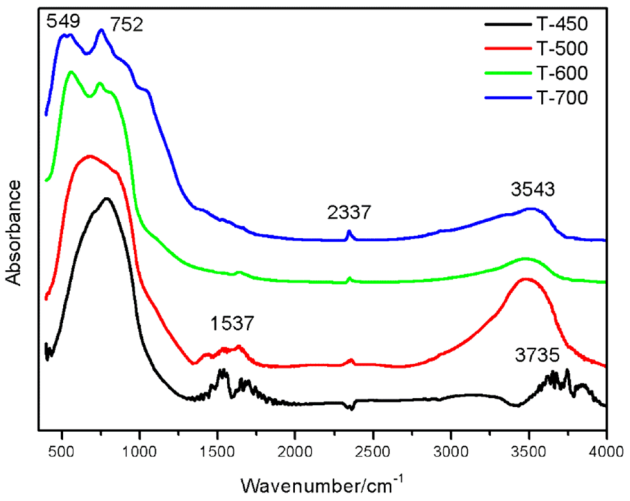

Fig. 2 FT-IR curves of T-450, T-500, T-600 and T-700

characteristics of hydroxyl groups at ~3543 cm^{-1} and hydrogen-bonded water molecules at ~3735 cm^{-1} [18, 19]. It is worth noting that the red shift in the 3000–4000 cm^{-1} range occurs when the annealing temperature rises, which signifies hydroxyl groups gradually dominate as the annealing temperature rising. Furthermore, the band intensity of T-500 is highest among all samples in the wavenumber range of 3000–4000 cm^{-1} suggesting that T-500 has the largest number of hydroxyl groups. In the range of 1200–2000 cm^{-1}, two absorption bands are observed at 1537 and 1670 cm^{-1} in the T-450 curve. They are assigned to carbonate peaks and hydroxyl groups bending vibrations, respectively [19], resulting from the incomplete combustion of organics and the absorbed water. The two peaks tend to damp as the temperature rising indicating organics decompose completely and absorbed water molecules decrease. As is well-known, the bands in the range of <1000 cm^{-1} are related to Al-O vibrations. A wide absorption band appears at 500–1000 cm^{-1} in the curve of T-450. While it broadens and finally splits into two peaks at 549 and 752 cm^{-1} with annealing temperature rising. The two bands correspond to Al–O–Al and Al–O stretching vibration peaks, respectively [20]. The phenomenon manifests that dangling bonds (i.e., Al–O–, O–Al–) are prone to couple each other to form Al–O–Al at higher annealing temperature. The coupling behavior is bound to decrease the number of dangling bonds, vacancies and other defects and further affects the dielectric properties.

Figures 3, 4 show the surface and cross-sectional morphologies of T-450, T-500, T-600 and T-700 samples. The SEM surface and cross-sectional morphologies reveal that there is no obvious change on the surface and cross-section among samples. The surface and cross-section are seen to be uniform and smooth without crystallization and crack (Fig. 3a–d) suggesting that films are amorphous. The surface topography of sample T-450 is observed by the AFM technology, as shown in Fig. 3e, f. The mean roughness of the T-500 is only ~1.4 nm suggesting that films are smooth.

4 Dielectric properties

Figure 5 shows the logJ–E characteristics of T-450, T-500, T-600 and T-700 with various ambient humidities. In the overall logJ–E curves, the current density increases in an ohmic way in the low electric field region, and then the escalation of current density slows down, saturates and even reduces in medium and high electric field region. However, the detail is not in complete accord. In the Fig. 5a, the leakage current density of T-450 shows strong dependence on the relative humidity that current density varies dramatically when they are exposed into different relative humidities. The maximum deviation caused by different ambient humidities is close to one order of magnitude at ~20 V. While the humidity dependence weakens as the annealing temperature rising. Namely, differing from the T-450, the current density distinction of samples which annealed at 500, 600 and 700 °C, respectively, shrinks gradually caused by various relative humidities, as shown in Fig. 5b–d. From the result of FT-IR, we have known that the T-450 has higher number of defects compared with the other samples. A large number of hydroxyl groups occupy defects through the Van der Waals force and hydrogen bond. They are more easily driven by strong electric field. Therefore, the leakage current density of T-450 presents the strong dependence on the relative humidity. While the dependence weakens owing to the coupling effect among dangling bonds as the temperature rising leading to defects decrease. For the reliability of amorphous alumina thin film, the films annealed above 450 °C should be reasonable. Moreover, the breakdown strength with different ambient humidities changes slightly. Namely, the ambient humidity scarcely makes positive effect on breakdown strength.

The annealing temperature effect on leakage current density and breakdown strength is analyzed. Figure 6 shows the logJ–E characteristics of T-450, T-500, T-600 and T-700 at the constant relative humidity of 20%. The leakage current densities of T-600 and T-700 are evident higher than that of T-450 and T-500 films in the electric field region of 0–200 MV/m. Typically, the leakage current density of T-600 is one order of magnitude higher than that of T-450 at ~75 MV/m. The result can be explained by the two following aspects. (a) That is due to microstructural change of the film. It is well-known that carriers can be absorbed and scattered by structural defects [21]. According to the results of FT-IR, T-450 and T-500 have large number of defects than T-600 and T-700. Namely, T-450 and T-500

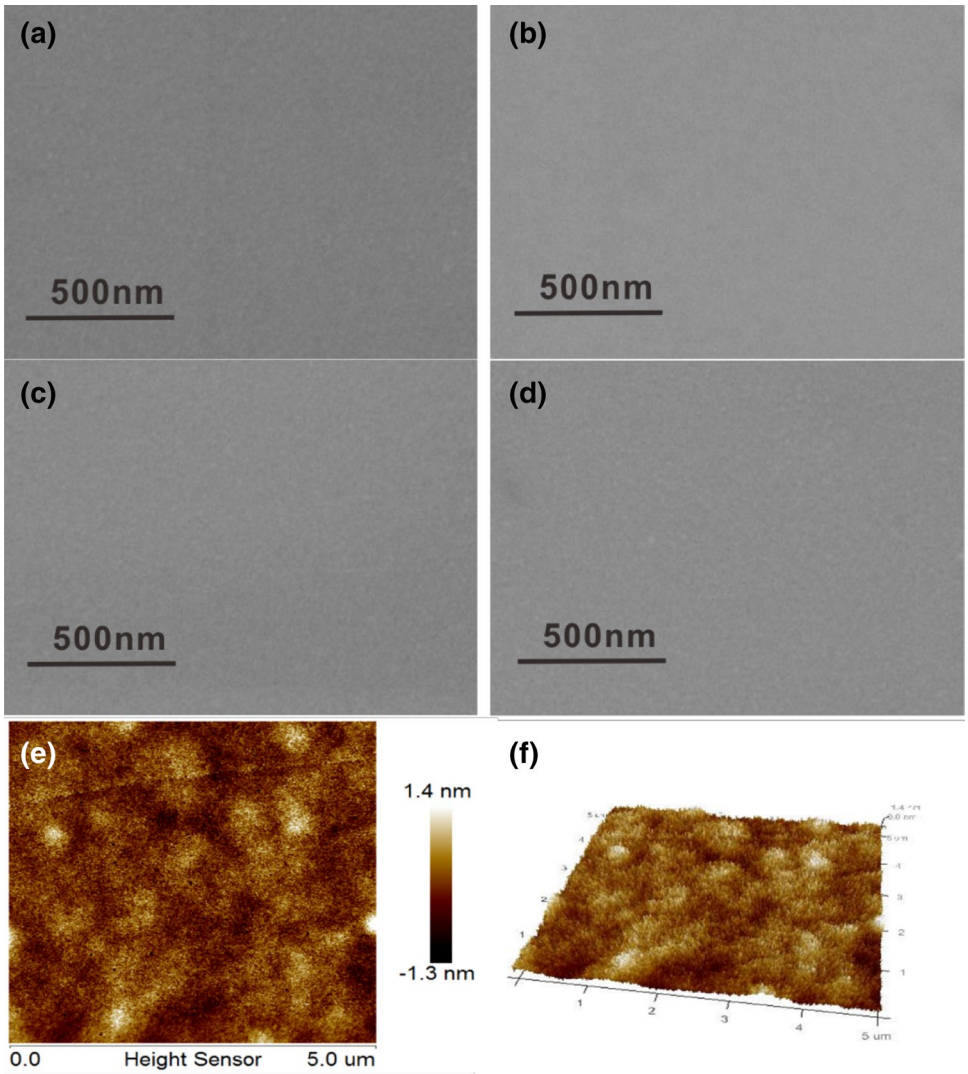

Fig. 3 Surface morphologies of **a** T-450, **b** T-500, **c** T-600 and **d** T-700; AFM **e** planar and **f** three-dimensional surface images of the T-500

possess more pronounced absorbing and scattering effect. Consequently, the leakage current densities of T-450 and T-500 are lower than that of the T-600 and T-700. (b) The crystal growth of platinum layer on the surface of Pt/Ti/SiO_2/Si substrate also is responsible for the phenomenon. Grain size and roughness of platinum increase as annealing temperature rising leading to the poor interfacial contact between platinum and alumina film. The poor contact results in the leakage current density increase. As is well known, the application of dielectrics needs the small leakage current density. Therefore, the annealing temperatures of 450 and 500 °C are expected to anneal the alumina thin film. From the view of breakdown strength, the breakdown strength values of all samples are similar which vary from 310 to 320 MV/m. The deviations are justified because numerous factors can influence breakdown strength, such as contact stress between probe and top electrode.

To get a deep insight into the annealing temperature effect on dielectric properties of alumina thin film, the frequency dependence of dielectric constant and dielectric loss tangent for alumina thin films which annealed at 450, 500, 600 and 700 °C, respectively, are analyzed in the frequency range from 200 kHz to 2 MHz at room temperature, as shown in Fig. 7. Obviously, the overall dielectric spectra are typical characteristics of conduction dominant low loss linear dielectrics. No apparent dielectric relaxation at room temperature is observed at low frequency range [17]. Moreover, both dielectric constant and dielectric loss decrease with the increase of frequency. The dielectric constant of T-500 decreases from 14.4 to 10.6, which is higher than that of the others in the whole frequency. The dielectric constant is related with dipoles polarization. Dipoles polarization is associated with the hydroxyl groups and absorbed water existing in films [16], and the T-500 has the largest number of hydroxyl groups, which has been proven by the FT-IR. Therefore, T-500 has the highest dielectric constant among samples. Meanwhile, the sample T-500 embraces a slightly higher dielectric loss at

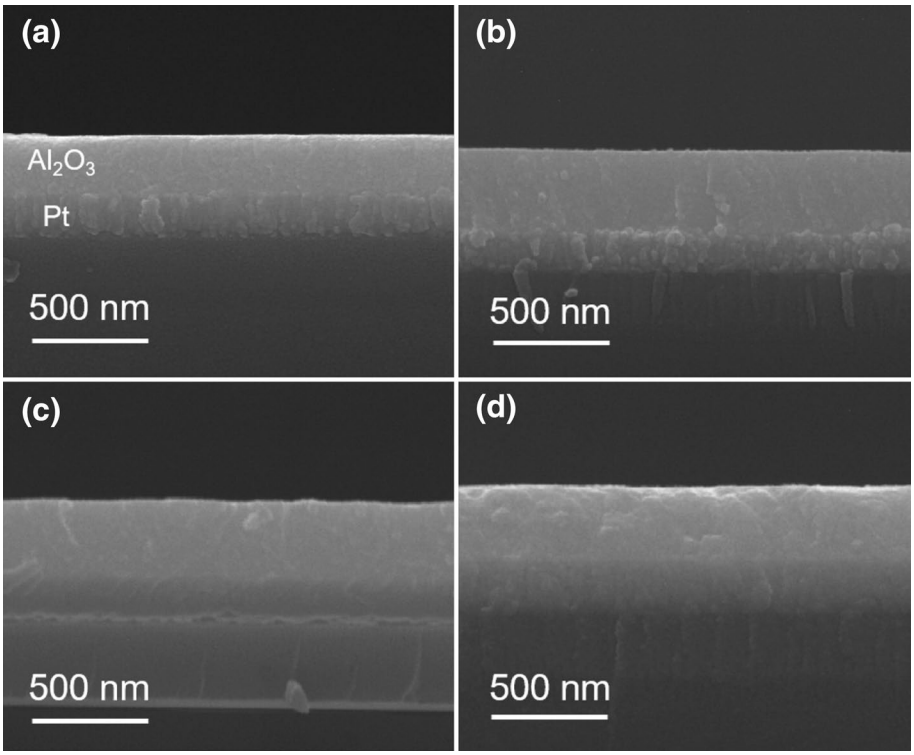

Fig. 4 The cross-sectional SEM images of **a** T-450, **b** T-500, **c** T-600 and **d** T-700

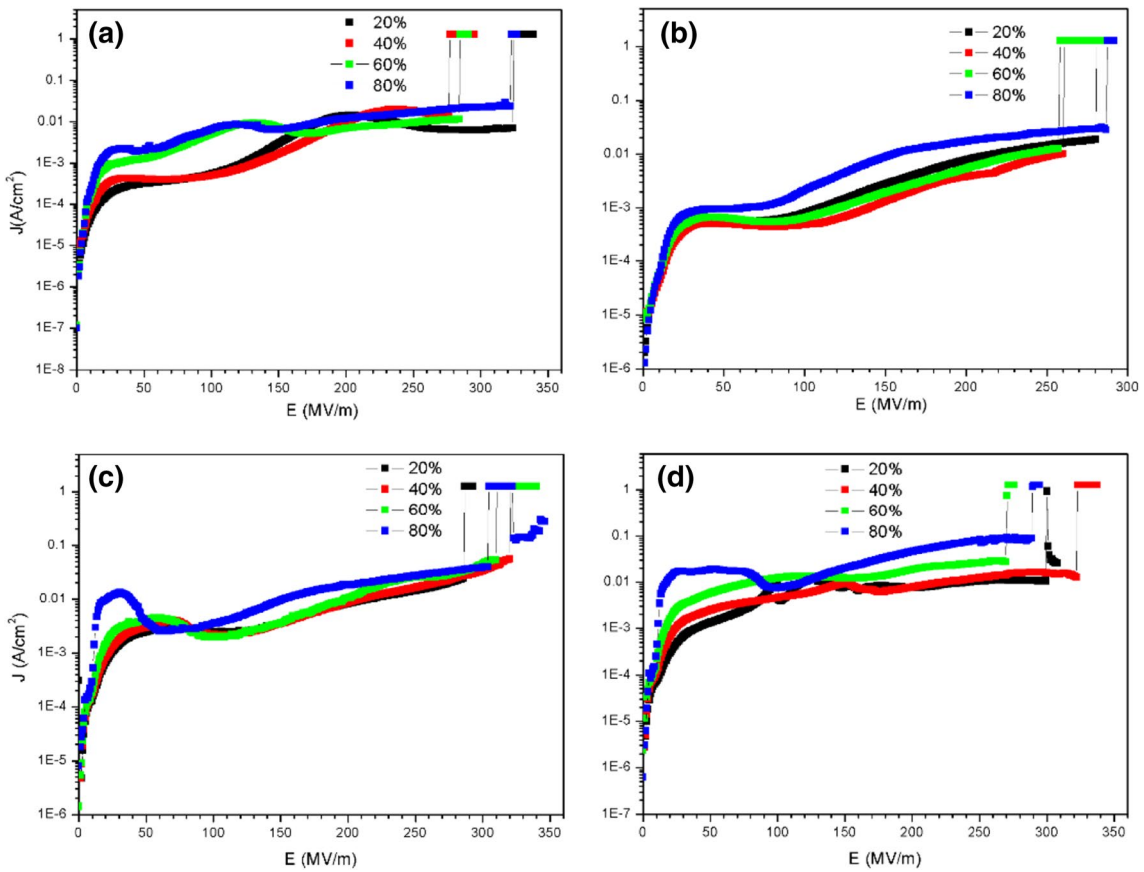

Fig. 5 The ambient humidity effect on logJ–E characteristics of **a** T-450, **b** T-500, **c** T-600, **d** T-700

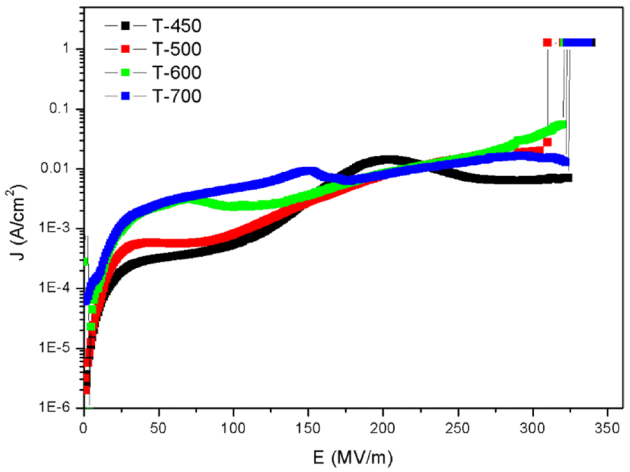

Fig. 6 The annealing temperature effect on logJ–E characteristics of T-450, T-500, T-600 and T-700 at the constant relative humidity of 20%

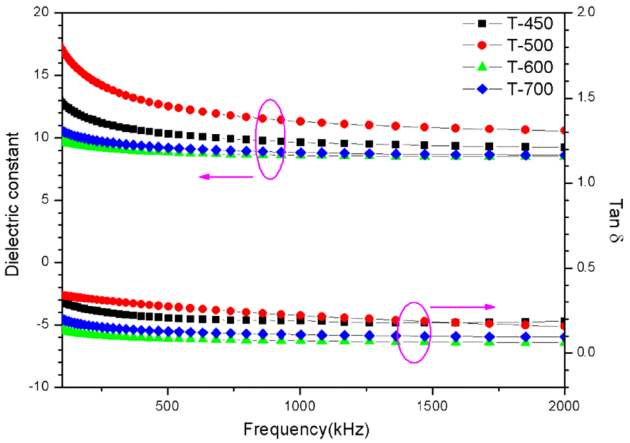

Fig. 7 Dielectric constant and dielectric loss of T-450, T-500, T-600 and T-700

low frequency. However, the distinct differences gradually decrease as the frequency increasing. The annealing temperature makes a minor contribution to dielectric loss but can enhance the dielectric constant at 500 °C. Moreover, dielectric constant and dielectric loss are stable in the range of 500 kHz–2 MHz. The frequency stability is an important parameter that determines the alumina thin film's suitable for electrical application.

In terms of effects of ambient humidity and annealing temperature on leakage current, breakdown strength, and dielectric constant and loss, the temperature of 500 °C should be chosen to anneal the alumina films.

According to the above result, the T-500 is considered as a typical sample, presenting excellent dielectric quality. The logJ–logE characteristics of T-500 in electric field of 0–360 MV/m at different environmental temperatures are displayed in Fig. 8. At the environmental temperature of 20 °C, the Ohmic conduction mechanism dominates the current density in the lower electric field (1–2 MV/m) [22]. In the electric field of 2–20 MV/m, the space charge limited currents mechanism mainly dominates current density owing to the linear behavior of logJ–logE [23], as shown in Fig. 8. However, the conduction mechanism is complicated in high electric field (>20 MV/m). It is generally estimated that space-charge-limited current, Schottky emission, and even other conduction mechanisms co-exist under high electric field [24]. Based on the previous paper [25], the conduction mechanism is generally deduced by the slope of logJ–logE curves or the variant (i.e., lnJ–lnE, Ln(J/E)-$E^{1/2}$). Obviously, the slope of curves present almost no evident change in the electric field of 0–70 MV/m, while the slope changes slightly above 70 MV/m. In general, the conduction mechanism of T-500 remains relatively stable at various ambient temperatures.

5 Conclusions

In conclusion, amorphous alumina thin films were deposited on Pt/Ti/SiO_2/Si substrates by sol–gel and spin-coating technology. Effects of annealing temperature, relative ambient humidity and temperature on dielectric properties of amorphous alumina thin films were further investigated. The annealing temperatures varied from 450 to 700 °C, the FT-IR results showed that dangling bonds coupled each other resulting in defects decrease with increasing of annealing temperature. The XRD and SEM results showed that all as-deposited films were dense and uniform without crystallization. Furthermore, the leakage current density of

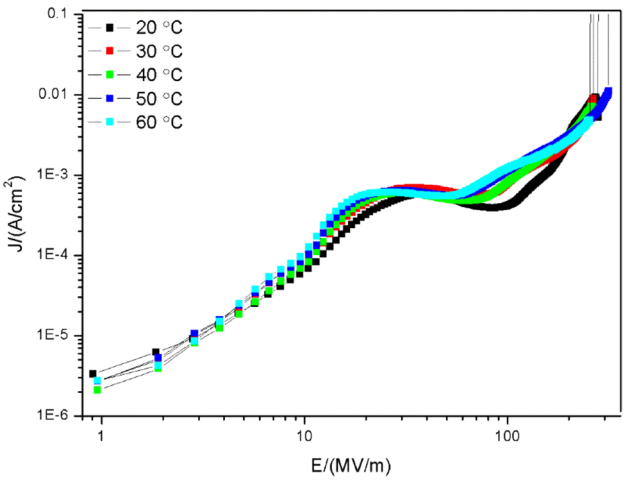

Fig. 8 Environmental temperature dependence of logJ–logE characteristics of the T-500

films annealed at 450 °C exhibited the strong dependence on the relative humidity, while the dependence weakened as the annealing temperature rising. And films annealed at 450 and 500 °C presented the lower leakage current densities than the films annealed at 600 and 700 °C at constant ambient humidity of 20%. Moreover, the dielectric constant of the film annealed at 500 °C was higher than the other samples. However, the dielectric loss changed slightly under various annealing temperatures conditions. Meanwhile, dielectric constant and loss almost remained unchanged in the frequency range from 500 kHz to 2 MHz. Reasonable annealing temperature of 500 °C was chosen, and the conduction mechanism for the films annealed at 500 °C was relatively stable with different ambient temperatures. Moreover, the annealing temperature, ambient humidity and temperature did not make the remarkable difference on the breakdown strength.

Acknowledgements This work is supported by the Ministry of Science and Technology of China through 973-project (Grant No. 2015CB654601) and National Science Foundation of China (Grant No. 51272177).

References

1. X. Nie, E.I. Meletis, J.C. Jiang, A. Leyland, A.L. Yerokhin, A. Matthews, Abrasive wear/corrosion properties and TEM analysis of Al_2O_3 coatings fabricated using plasma electrolysis. Surf. Coat. Technol. **149**, 245–251 (2002)
2. A.C.M. Esther, N. Sridhara, S.V. Sebastian et al., Optical and RF transparent protective alumina thin films. J. Mater. Sci. **26**, 9707–9716 (2015)
3. G. Ortega-Cervantez, G. Rueda-Morales, J. Ortiz-Lopez, Cold-wall CVD carbon nanotube synthesis on porous alumina substrates. J. Mater. Sci. **20**, 403–407 (2009)
4. C.L. Huang, J.J. Wang, F.S. Yen, C.Y. Huang, Microwave dielectric properties and sintering behavior of nano-scaled (α+θ)-Al_2O_3 ceramics. Mater. Res. Bull. **43**, 1463–1471 (2008)
5. B. Soltani, M. Babaeipour, A. Bahari, Studying electrical characteristics of Al_2O_3/PVP nano-hybrid composites as OFET gate dielectric. J. Mater. Sci. (2016). doi: 10.1007/s10854-016-6064-2
6. D.D. Marco, K. Drissi, N. Delhote, O. Tantot, P.M. Geffroy, S. Verdeyme, T. Chartier, Dielectric properties of pure alumina from 8 GHz to 73 GHz. J. Eur. Ceram. Soc. **36**, 3355–3361 (2016)
7. N.H. Fletcher, A.D. Hilton, B.W. Ricketts, Optimization of energy storage density in ceramic capacitors. J. Phys. D **29**, 253–258 (1996)
8. A. Boumaza, L. Favaro, J. Lédion, G. Sattonnay, J.B. Brubach, P. Berthet, A.M. Huntz, P. Roy, R. Tétot, Transition alumina phases induced by heat treatment of boehmite: an X-ray diffraction and infrared spectroscopy study. J. Solid. State. Chem. **182**, 1171–1176 (2009)
9. Y.W. Li, Q. Qiao, Z. Dong, J.Z. Zhang, Z.G. Hu, J.H. Chu, Enhanced dielectric properties in bismuth-doped alumina films prepared by atomic layer deposition. J. Non-Crysta. Solid. **443**, 17–22 (2016)
10. P.J. Kelly, R.D. Arnell, Control of the structure and properties of aluminum oxide coatings deposited by pulsed magnetron sputtering. J. Vac. Sci. Technol. A **17**, 945–953 (1999)
11. M.S. Al-Robaee, G.N. Subbanna, K.N. Rao, S. Mohan, Studies of the optical and structural properties of ion-assisted deposited Al_2O_3 thin films. Vacuum **45**, 97–102 (1994)
12. A.K. Dua, V.C. George, R.P. Agarwala, Characterization and microhardness measurement of electron-beam-evaporated alumina coatings. Thin Solid Films **165**, 163–172 (1988)
13. J.B. Kim, D.R. Kwon, K. Chakrabarti, C. Lee, K.Y. Oh, J.H. Lee, Improvement in Al_2O_3 dielectric behavior by using ozone as an oxidant for the atomic layer deposition technique. J. Appl. Phys. **92**, 6739–6742 (2002)
14. M.T. Aguilar-Gama, E. Ramírez-Morales, Z. Montiel-González, Structure and refractive index of thin alumina films grown by atomic layer deposition. J. Mater. Sci. **26**, 5546–5552 (2015)
15. A.W. Ott, J.W. Klaus, J.M. Johnson, S.M. George, Al_2O_3 thin film growth on Si(100) using binary reaction sequence chemistry. Thin Solid Films **292**, 135–144 (1997)
16. M. Yao, P. Zou, Z. Su, J.W. Chen, X. Yao, The influence of Yttrium on leakage current and dielectric properties of amorphous Al_2O_3 thin film derived from sol-gel. J. Mater. Sci. **27**, 7788–7794 (2016)
17. M Yao, Z Su, P Zou, J.W. Chen, F Li, X. Yao, Dielectric properties under high electric field for silicon doped alumina thin film with glass-like structure derived from sol-gel process. J. Alloy. Compd. **690**, 249–255 (2017)
18. A.A. Hind, V.H. Grassian, FT-IR study of water adsorption on aluminum oxide surfaces. Langmuir **19**, 341–347 (2002)
19. L.A. Phillips, G.B. Raupp, Infrared spectroscopic investigation of gas-solid heterogeneous photocatalytic oxidation of trichloroethylene. J. Mol. Catal. **77**, 297–311 (1992)
20. D.N. Goldstein, J.A. Mccormick, S.M. George, Al_2O_3 atomic layer deposition with trimethylaluminum and ozone studied by in situ transmission FT-IR spectroscopy and quadrupole mass spectrometry. J. Phys. Chem. C **112**, 19530–19539 (2008)
21. S. Ahmad, A. Ibrahim, R. Alias, S.M. Shapee, Z. Ambak, S.Z. Zakaria, M.R. Yahya, Thermal and electrical characterization of alumina substrate for microelectronic applications. AIP Conf. Proc. **1217**, 442–446 (2010)
22. H. Birey, Dielectric properties of aluminum oxide films. J. Appl. Phys. **45**, 2898–2904 (1978)
23. A. Rose, Space-charge-limited currents in solids. Phys. Rev. **97**, 1538–1544 (1955)
24. Y. Peng, M. Yao, R. Xiao, X. Yao, Electrical properties of sol-gel derived Mg-doped Al_2O_3 films. J. Mater. Sci. **27**, 11495–11501 (2016)
25. S.K. Sahoo, R.P. Patel, C.A. Wolden, Leakage current mechanisms in high performance alumina-silicone nanolaminate dielectrics. Appl. Phys. Lett. **101**(1–4), 142903 (2012)